Multi-participant operation optimization for charging systems with orderly charging and cooperative game strategies considering carbon capture and uncertainties

Lin, Hongyu; Han, Xingbang ; Yu, Pengshuo ; Yan, Qingyou ; Yang, Shenbo ; Shi, Mengshu ; Anvari-Moghaddam, Amjad; Liang, Dong

Published in:
Journal of Energy Storage

DOI (link to publication from Publisher):
10.1016/j.est.2022.106471

Publication date:
2023

Document Version
Accepted author manuscript, peer reviewed version

Multi-participant operation optimization for charging systems with orderly charging and cooperative game strategies considering carbon capture and uncertainties

Hongyu Lin[1,2,*], Xingbang Han[3], Pengshuo Yu[1,2], Qingyou Yan[1,2], Shenbo Yang[4,*], Mengshu Shi[1,2], Amjad Anvari-Moghaddam[5], Dong Liang[6]

1 School of Economics & Management, North China Electric Power University, Beijing 102206, China

2 Beijing Key Laboratory of New Energy & Low Carbon Development, North China Electric Power University, Beijing 102206, China

3 School of Humanities and Social Sciences, North China Electric Power University, Beijing 102206, China

4 College of Economics and Management, Beijing University of Technology, Beijing 100124, China

5 Department of Energy (AAU Energy), 9220 Aalborg, Denmark

6 State Grid Jibei Electric Power Company Limited, Beijing 10054, China

* Corresponding Author

ABSTRACT: In order to further enhance the utilization rate of renewable energy and achieve the goal of carbon emission reduction, this paper establishes a stable and clean energy supply mode of charging system and constructs a three-stage optimization and benefit distribution model. Firstly, the charging system structure is built with employing photovoltaic generator and carbon capture thermal power generator. Secondly, the charging load uncertainty is modelled by using Markov Chain where the differences of speeds of vehicles are considered. Thirdly, a deterministic charging optimization model is constructed in the first stage, with the objectives of economy, environment, energy utilization and load fluctuation; and then, in the second stage, the uncertainty of photovoltaic power generation is considered to formulate two types of information gap decision theory-based models. Finally, a double factor-involved benefit allocation model for the proposed charging system is constructed in the third stage, based on the Shapley method. The case study shows that: (1) the forecast error of charging load is smaller by considering quantity transfer and speed differences; (2) carbon capture and storage system reduces CO_2 emission by 85.08% and system's cost by 2.60%; (3) Tripartite cooperation maximizes the system's benefits, and IGDT provides multiple strategies for dealing with PV uncertainty; (5) benefit allocation considering economy and environment is more rational and highlights the contribution of carbon capture system.

KEYWORDS: Electric vehicles; carbon capture; uncertainties; Markov chain; information gap decision theory; multi-factor Shapley

1 Introduction

1.1 Motivation

With the increasing proportion of renewable energy generation, the uncertainty has a certain impact on the safety and stability of the power grid, which makes large-scale grid connection of renewables a difficult problem [1]. Volatility and randomness of renewable energies can be solved through the auxiliary service of traditional generators [2]. The capacity of thermal power in China still accounts for a large proportion in the short term, so it is necessary to make full use of thermal power for auxiliary services [3]. However, traditional thermal power has a large amount of carbon dioxide emissions, which has a negative impact on the environment. With the proposal of China's carbon reduction goal, the electric power industry is a key target of carbon emission reduction. Carbon capture technology is an effective means to alleviate the contradiction between fossil fuel utilization and carbon emission reduction [4]. Therefore, it is of importance to construct a **stable and clean** system by applying the carbon capture technology to thermal power generators in the system.

On the other hand, insufficient consumption of renewable energies leads to a large number of resources waste. Electric vehicle (EV) charging excels at enhancing renewable energy consumption, but large-scale EV charging may cause peak superposition, and thus jeopardize the operation of grid [5]. Therefore, it is urgent to conduct a study on motivating users to ordered charge according to the output of renewable energy, so as to achieve **peak shaving** and **increase renewable energy consumption**.

Above all, this paper aims to construct an optimization model for charging system operation considering carbon capture and source-load uncertainties. Moreover, a fair benefit allocation strategy is proposed to incentivize multiple entities for participation.

1.2 Literature review

For uncertainty modelling of charging load, according to the travel characteristics of EVs, the position transfer state at the next time point is only affected by the position state at the current time point and has nothing to do with the past, which is in line with the Markov attribute [6]. Therefore, Markov Chain can be used to predict the transfers of EVs in time and space. The works of [7-12] have already verified the positive effects of Markov Chain on addressing uncertainty of charging load. Therein, Yan et al. [11] also simulated and forecast charging load by using Markov chain, and traffic jam and weather were taken into consideration; In the work of Han et al. [12], the numbers of chargeable EVs in different types of areas were taken as a factor to describe the behavior characteristics of EVs. **These studies characterize the individual differences of EVs from the perspectives of location transfer, travel time, dwelling time, and driving mileage, but they all ignore an important factor, that is, the driving speed. Energy**

consumption of EVs is different at different driving speeds, so it also needs to be considered in the process.

After addressing the load uncertainty, research on the operation optimization of charging system is carried out. The works of [12-17] has contributed a lot of research achievements on this topic. Among them, Han et al. [12] carried out an ordered charge control to reduce peak-valley difference and renewables consumption. Borray et al. [13] optimized charging load with solar photovoltaic (PV) as power supplier, considering low-voltage network's constraints, and the aim was to increase the consumption of PVs. Climent et al. [14] proposed an energy management strategy for a plug-in parallel hybrid EV with the goal of minimizing the fuel consumption while fulfilling the constraint on the terminal battery SOC. **However, these literatures did not consider an important premise, i.e., the stability of the system. Neither the impact of the renewable energy's uncertainty on the system was considered, nor the energy supply structure of "renewable energy + traditional auxiliary generators" was established.**

Regarding research on the uncertainty of renewable energy, most of the works used probabilistic decision-making methods [18-20] and fuzzy decision-making methods [21, 22]. The probability decision-making method needs numerous data to fit the accurate probability distribution, which has certain requirements for the fitting accuracy. Fuzzy decision-making methods have large subjectivity, and it is not easy to balance the subjective and objective weights. Different from the above methods, information gap decision theory (IGDT) presupposes the acceptable deviation range of decision makers, maximizes the adverse disturbance under this premise, and obtains the acceptable deviation results, as the work of Wei et al. demonstrated [23]. The method can not only get the robust optimal solution, but also get the optimal profit at the preset opportunity income level [23]. Currently, this theory was applied in numerous papers for modeling the uncertainty of renewable energies, where its effectiveness was verified, including the works of [24], [25], and [26]; **however, the positive effect of IGDT on charging systems in identifying uncertainty risk has not been studied in these papers.**

The system's stability is not only reflected in the process of wind and solar uncertainty modeling, but also reflected in the construction of charging systems with traditional stable power generators involved. Such systems usually use traditional thermal power units for peak shaving or standby [3], which will produce a large number of carbon dioxide emissions. Carbon capture and storage (CCS) technology is an effective way to realize low carbonation in power industry. By equipping thermal power units with carbon capture system, the carbon emission intensity can be significantly reduced and the flexibility of units can be improved [27]. Zhang et al. [28] constructed an integrated energy system where CCS system and power-to-gas were employed, and the superiority of CCS technology in environmental and economic benefits was proved. Taljegard et al. [29] applied a cost-minimization investment model and an electricity dispatch model of the Scandinavian and German electricity systems, assuming both optimized charging and a vehicle-to-grid charging strategy. Cao et al. [30] built a novel integrated electricity-gas system with power-to-gas, carbon capture thermal power (CCTP) and EVs, to minimize operating costs,

reduce CO_2 emissions, and improve utilization efficiency of wind power. As auxiliary generators, CCTP may earn less than renewable energies. **Since visible benefits are an incentive for such entity to participate in joint operation, it is necessary to study scientific and reasonable distribution strategies.**

The Shapley method can solve the problem that many entities have conflicts in the process of cooperation due to the distribution of interests, and one of the advantages is to distribute the benefits according to the marginal contribution rate of members to the alliance [31]. Wang et al. [32] applied game theory to the multi-agent capacity optimization model with basic Shapley method involved; Fang et al. [33] improved the conventional Shapley method according to the players' characteristics; Tan et al. [34] combined Shapley method with nucleolar method to deal with the distribution between power suppliers and users in a virtual power plant; Yang et al. [35] improved basic Shapley method by introducing risk factor to propose an income distribution strategy for park integrated energy systems. Yang et al. [36] introduced cost factor and contribution factor to their former improved Shapley method. **Researchers have already demonstrated the effectiveness of the Shapley-based benefit allocation, but they barely considered the environmentally relevant factor to improve the basic method, since carbon emission reduction is a trend to pursue.**

1.3 Research gap

In light of the literature review, some points did not be considered which are shown below:

(1) Few studies mention the factor of driving speed when considering the individual differences of charging users in the process of quantity transfer modeling based on Markov Chain;

(2) In the research on charging strategy, there is a lack of consideration of system stability. The stability and flexibility of the charging system constructed by the existing literature are weak: On the one hand, there is no stable generator as auxiliary support (let alone the cleanliness of the auxiliary unit); On the other hand, the impact of uncertainties of renewables was not studied in such charging system.

(3) Scientific and reasonable benefit allocation in a stable and clean charging system was not studied. Most papers either only consider the economic benefit distribution, or involve many factors and propose a novel distributed method but without mentioning environmental factor, which is unfavorable to the CCTP generators.

1.4 Contributions

The possible contributions are illustrated from three perspectives, which are shown below:

- In terms of load side:

  On the basis of the consideration of quantity transfer, the uncertainty of charging load is also modeled with considering the differences of driving

speed. The numbers of charging users in work area and home area are obtained through Markov Chain based on the data of NHTS 2017; At the same time, the factor of speed differences is introduced, and the daily mileage curve is re-fitted based on the data of EV users (the fitting results are better than the work of Han et al. [12]). The charging load curve established by the proposed method is better than the result generated by Monte Carlo and that of Han et al.

- In terms of source side:
  In order to reduce the interference of PV's fluctuation and randomness, the IGDT is used to deal with the uncertainty of PV. In the IGDT-based optimization model, decision makers are divided into pessimists and optimists. Based on the deterministic model, the maximum PV deviation and the minimum PV deviation are respectively taken as the objectives, the ranges of acceptable benefit variation are added as new constraints, and thus the risk aversion strategy and opportunity pursuit strategy are proposed. The proposed model provides a new idea for the research direction of uncertainty in the operation optimization of charging systems.
- In terms of the whole system:
  A stable and clean EV charging system is constructed, an optimization model for the system is established, and a double-factor Shapley method is proposed for the system. In this paper, an energy supply structure of "PV+CCTP" is proposed, and a multi-objective optimization model including the aims of economic benefits, emission reduction, renewable energy utilization and load fluctuation is established. A benefit allocation strategy is proposed considering economy and environment, so as to make the income of each participant more reasonable and incentivize the participants, which provides a reference for the new power system with carbon capture thermal power employed to enhance the operation vitality.

1.5 Organization of this paper

The rest of this paper is organized as follows and shown in Fig. 1. Section 2 introduces the structure of charging system in this paper, and then models the uncertainty of charging load based on Markov chain. In Section 3, a charging optimization model without considering PV uncertainty is constructed, and the proposed model in this section is considered as the first-stage model. Section 4 builds an IGDT-based model, and this section is the second stage of optimization. Section 5, i.e., the third stage, introduces a cooperative game, and allocates the optimized benefits among the participants based on the Shapley-value method. An example analysis is conducted in Section 6, and conclusions are drawn in Section 7.

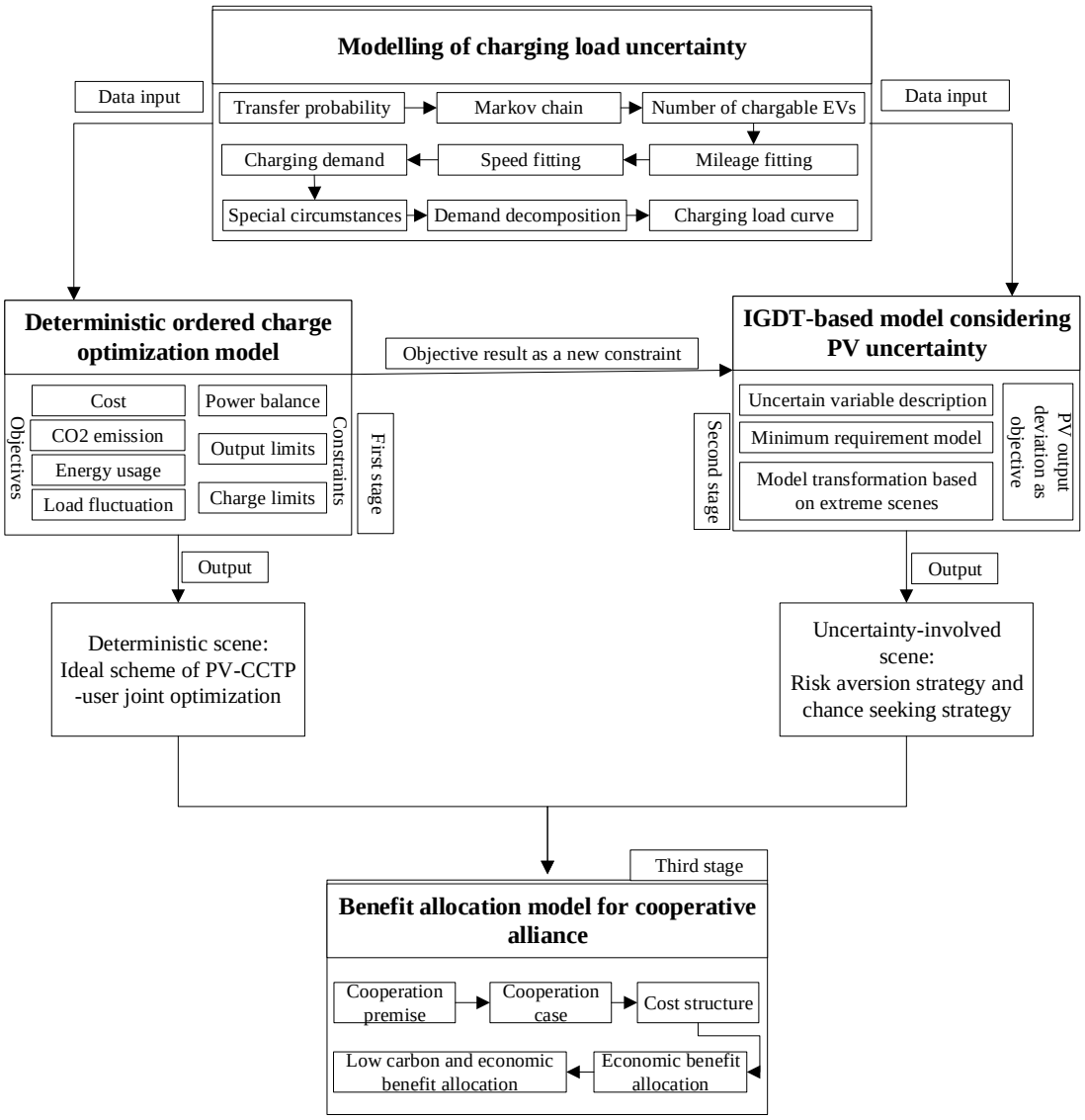

Fig. 1 Organization of this paper

2 Charging system structure and load uncertainty modelling

2.1 Charging system structure

The charging system mentioned in this paper mainly includes three participants: PV, CCTP, and EV users (shown in Fig. 2). The charging load of EVs is first satisfied by the PV in the system. When the charging demand exceeds the output of PV, the CCTP is employed as a supplement.

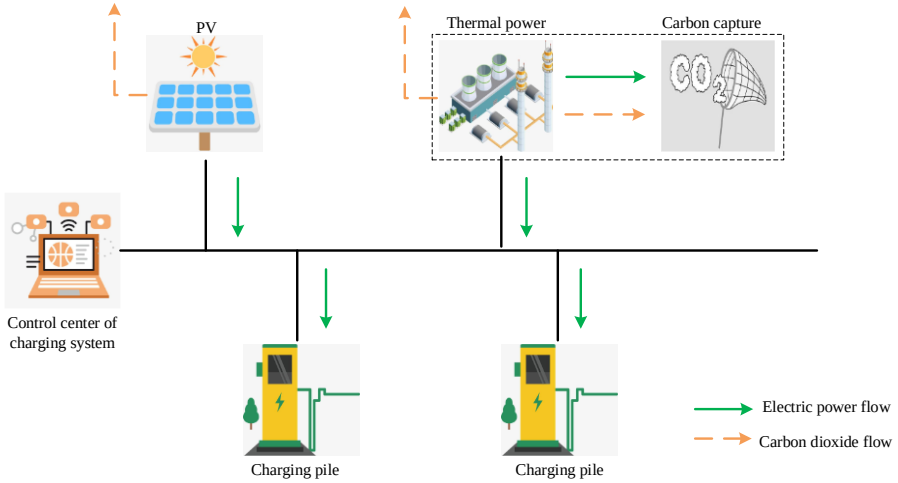

Fig. 2 System structure

2.2 Construction of quantity forecasting model for EVs

2.2.1 Modelling of Markov Chain [6]

In a process, the state of each time point is random, and the future state is not limited by the past state, but only related to the current state. The current state of an EV is set as S_t, the next state is S_{t+1}, and then the conditional probability of Markov Chain is formulated as follows:

$$P(S_t \rightarrow S_{t+1}) = P(S_{t+1} \mid S_1, S_2, S_3, ..., S_t) = P(S_{t+1} = j \mid S_t = i) = p_{ij} \tag{1}$$

where p_{ij} is the transfer probability of an EV from time t to t+1; herein, i is the position state at time t, and j is the position state at time t+1. According to the data of the national household travel survey (NHTS), electric vehicle destinations can be divided into home (H), work (W) and other (O) areas. The position transfer frequency matrix $M_{t,t+1}$ is given by

$$M_{t,t+1} = \begin{bmatrix} N_t / N_{t+1} & s_h & s_o & s_w \\ s_h & n_{h,h} & n_{h,o} & n_{h,w} \\ s_o & n_{o,h} & n_{o,o} & n_{o,w} \\ s_w & n_{w,h} & n_{w,o} & n_{w,w} \end{bmatrix} \tag{2}$$

Where N_t and N_{t+1} are the states of time t and time t+1, s_h, s_w, and s_o are the states of EVs who arrive at H, W, and O areas respectively, and $n_{a,b}$ is the number of EVs who transfer from area a to area b.

Then, transition probability can be calculated according to the following equation (Taking $p_{h,w}$ as an example).

$$p_{h,w} = \frac{n_{h,w}}{n_{h,h} + n_{h,w} + n_{h,o}} \tag{3}$$

where $p_{h,w}$ is the probability of EVs transferring from H to W. In the same way, we can obtain the transfer probability matrix $P_{t,t+1}$ as follows.

$$P_{t,t+1} = \begin{bmatrix} p_{h,h} & p_{h,o} & p_{h,w} \\ p_{o,h} & p_{o,o} & p_{o,w} \\ p_{w,h} & p_{w,o} & p_{w,w} \end{bmatrix} \tag{4}$$

After K transitions, the state probability distribution can be obtained according to the following equation.

$$P(k) = P_0 P_{t,t+1}^k \tag{5}$$

where P_0 is the original number of EVs.

2.2.2 Forecasting process

The quantities of EVs in different areas are predicted according to the following steps [12]:

Step 1: filter and process the travelling data of EVs;

Step 2: set that the target time range is one day, and the day is divided into 24 measuring points (t=1, 2, 3, …,24), and determine the original numbers of EVs;

Step 3: calculate the transfer frequency matrix;

Step 4: calculate the transfer probability matrix;

Step 5: verify whether the collected data has Markov properties by calculating the boundary probability P_j (given by eq. (6)) and then using chi-square statistic (given by eq. (7)).

$$P_j = \frac{\sum_{i=1}^{I} n_{ij}}{\sum_{j=1}^{J}\sum_{i=1}^{I} n_{ij}} \tag{6}$$

$$\chi^2 = 2\sum_{j=1}^{J}\sum_{i=1}^{I} n_{ij} \left| \log \frac{P_{ij}}{P_j} \right| \tag{7}$$

Step 6: predict the quantities of EVs.

2.3 Charging load model construction

(1) daily mileage fitting

According to the experience, the mileage of each travel meets the lognormal distribution, which is given by

$$d = \frac{1}{x\sigma\sqrt{2\pi}} \cdot e^{-\frac{(\ln x-\mu)^2}{2\sigma^2}} \tag{8}$$

where μ and σ are the expected value and standard deviation.

(2) SOC

SOC is the ratio of electricity quantity to rated power, which is given by

$$SOC_i = \frac{E_i}{E_{bat}} \tag{9}$$

where E_i could be remaining capacity and power consumption, denoted as E_{rem} and E_{char}, and the SOCs corresponding to remaining, and chargeable amounts, are denoted as SOC_{rem} and SOC_{char}.

(3) The relationship between vehicle speed and unit power consumption

According to the work of [37], the unit energy consumption model of EVs is related to speeds, which is given by

$$e = 0.21 - 0.001v + \frac{1.531}{v} \tag{10}$$

where v is the speed.

(4) energy consumption function

$$E_{pc} = \frac{d \cdot e}{\varepsilon} \tag{11}$$

where E_{pc} is the power consumption of an EV, d is the mileage, e is the unit power consumption, and ε is the consumption efficiency.

(5) Charging duration

$$T_L = \frac{E_{char}}{p_e} = \frac{E \cdot (0.95 - SOC_{rem})}{p_e} \tag{12}$$

where T_L is the charging duration, p_e is the charging power, and E is the rated capacity.

(6) Charging load decomposition

The total charging demand of an EV is decomposed within its charging duration, which is given by

$$P_{EV,t} = \sum_{i=1}^{N} P_{i,t} \tag{13}$$

where $P_{EV,t}$ is the charging power of the charging system at time *t*, $P_{i,t}$ is the charging power of EV *i* at time *t*, and N is the number of EVs.

3 First stage - charging optimization model without considering the uncertainty of PV

3.1 Output models of generators

(1) CCTP

Through capturing and storing carbon dioxide emitted by traditional thermal power, carbon dioxide emissions are reduced. Structure and operation introductions of CCS are detailed in the work of [38]. In the operating process of a CCS system, the total energy consumption mainly comes from the operating energy consumption of each link [39]. The relationship between unit output and operating energy consumption is shown below:

$$P_t^{net} = P_t^{out} - P_t^{ec} \tag{14}$$

$$P_t^{ec} = P^f + P_t^v \tag{15}$$

where P_t^{net}, P_t^{out}, and P_t^{ec} are respectively the net power generation, equivalent power output, and energy consumption for carbon capture, P^f and P_t^v are the fixed energy consumption and operating energy consumption (i.e., energy consumption for carbon capturing). P_t^v is calculated by

$$P_t^v = m^c E_t^{CO2} \tag{16}$$

where m^c is the operation energy consumption for capturing a unit of CO_2, E_t^{CO2} is the amount of CO_2 being captured at time *t*.

Emitted CO_2 from thermal power generation E_t^G minus the CO_2 collected by CCS E_t^R equals net carbon emissions of CCTP E_t^{net}, which is given by

$$E_t^{net} = E_t^G - E_t^R \tag{17}$$

where E_t^G consists of the carbon emission intensity of thermal power e^g and power generation of CCTP P_t^{out}, and E_t^R is made up of CO_2 capture rate e^y and the collected

CO_2 (the capture rate usually is between 80%-95%). The equations are shown below.

$$\begin{cases} E_t^G = e^g P_t^{out} \\ E_t^R = e^y E_t^{CO2} \end{cases} \tag{18}$$

(2) PV

The PV output model generally coincides with the β distribution, which is detailed in the work of Tan et al. [20].

3.2 Objective functions

In addition to smoothing the charging load curve, this paper also intends to conduct an optimization from the 3E aspects, i.e., economy, environment, and energy usage. Economic benefits include users' cost C_{user}, PV's cost C_{pv}, and CCTP's cost (the details of each entity's cost are mentioned in section 5); Environmental benefits include CO_2 emission of CCTP q_{tu}; Energy use benefits include energy abandonment of PV e_{pv}.

(1) Minimizing the total cost of the system

$$f_1 = \min(C_{pv} + C_{tu} + C_{user}) \tag{19}$$

(2) Minimizing the total emissions of the system

$$f_2 = \min q_{tu} \tag{20}$$

(3) Minimizing the total energy abandonment

$$f_3 = \min e_{pv} \tag{21}$$

(4) Minimizing the load fluctuation

$$f_4 = \min\left(\frac{1}{T}\sum_{t=1}^{T}(P_t - \overline{P})^2\right) \tag{22}$$

where $\overline{P}$ is the daily average load, and $\overline{P} = \frac{1}{T}\sum_{t=1}^{T} P_t$.

(5) Multi-objective transferring to a single objective

The multiple objectives are integrated into a single objective function by weighing each objective, which is given by

$$\psi = w_1 \cdot f_1^{'} + w_2 \cdot f_2^{'} + w_3 \cdot f_3^{'} + w_4 \cdot f_4^{'} \tag{24}$$

where ψ is the transferred function, and $w_i, i = 1,2,3,4$ is the weight of the *i*-th function. In this paper, the weight of each objective is set to be 0.25.

3.3 Basic constraints

(1) Power balance

$$\sum_{i=1}^{\mathrm{NG}} g_{i,\mathrm{g}} + \sum_{m=1}^{\mathrm{NPV}} g_{m,\mathrm{pv}} = D \tag{25}$$

where $g_{i,\mathrm{g}}$ is the active power of CCTP i, $g_{m,\mathrm{pv}}$ is the active power of PV m, and D is the charging demand.

(2) Distribution transformer capacity constraints

$$P_t - P_{PV,t} < P_{MTF} \tag{26}$$

$$P_{MTF} = C_{MTF} \cdot \iota \cdot \tau \tag{27}$$

where P_t is the charging load, $P_{PV,t}$ is the dispatchable output of PV, P_{MTF} is the maximum bearing capacity of distribution transformer, C_{MTF} is the rated capacity of transformer, ι is the power factor, τ is the efficiency.

(2) Output constraints

The output of the generators shall not exceed the rated range. For PV:

$$g_{m,\mathrm{pv}}^{\min} \le g_{m,\mathrm{pv}} \le g_{m,\mathrm{pv}}^{\max} \tag{28}$$

where $g_{m,\mathrm{pv}}^{\max}$ and $g_{m,\mathrm{pv}}^{\min}$ are the maximum and minimum dispatchable outputs of PV m, respectively. For CCTP:

$$g_{i,\mathrm{g}}^{\min} \le g_{i,\mathrm{g}} \le g_{i,\mathrm{g}}^{\max} \tag{29}$$

where $g_{i,\mathrm{g}}^{\max}$ and $g_{i,\mathrm{g}}^{\min}$ are the dispatchable output bounds of CCTP i, respectively. In addition, the carbon capture capacity should also be within the rated range, i.e.,

$$e_{i,\mathrm{g}}^{\min} \le e_{i,\mathrm{g}} \le e_{i,\mathrm{g}}^{\max} \tag{30}$$

where $e_{i,\mathrm{g}}$, $e_{i,\mathrm{g}}^{\max}$, and $e_{i,\mathrm{g}}^{\min}$ are the amount of captured CO_2, maximum and minimum rated powers.

(3) Safe storage constraint

The battery has bounds for safe storage to avoid damages from over charging or low power, which is given by

$$E_{ra} \cdot \xi \le E_n \le E_{ra} \cdot \zeta \tag{31}$$

where E_n is the amount of stored electricity, E_{ra} is the rated power, ζ and ξ are the safe storage bounds.

(4) Charging power constraint

The charging power of EVs cannot exceeds the rated bounds, i.e.,

$$P_{t,\min} \le P_t \le P_{t,\max} \tag{32}$$

where $P_{t,\max}$ and $P_{t,\min}$ are the maximum and minimum charging powers.

(5) Charging duration constraint

The charging hours should be within the expected time so as to ensure the regular car usage, i.e.,

$$T_{\text{char}} \le T_{\text{exp}} \tag{33}$$

where T_{char} is the actual charging hours, and T_{exp} is the end time of charging users expect.

3.4 Solving algorithm

The proposed optimization model is solved by using the chaotic particle swarm optimization algorithm (CPSO). The basic particle swarm optimization (PSO) has a fast convergence speed, but it is easy to fall into the local optimum; therefore, the ergodicity of chaos idea is introduced into the PSO to solve the problem. In the process of particle iterative optimization, chaotic mapping is used to enrich the diversity of the particle population and improve the global search ability of particles, thus forming a CPSO. In the CPSO, the particle search is ergodic and does not experience all the states in the space repeatedly, so as to overcome the weakness of particles falling into the local extremum [40]. The algorithm principle is introduced in [41], and the solving steps are represented in Fig. 3 [42].

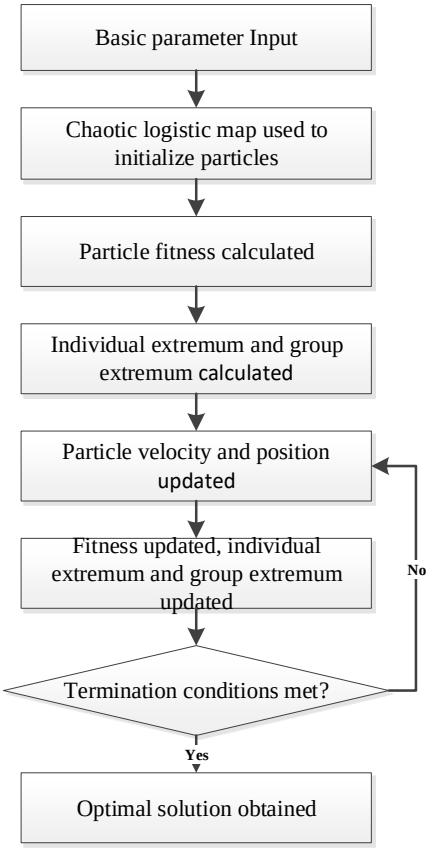

Fig. 3 Solving steps

3.5 Orderly charging process

Users access the charging system and input relevant information, including start time, departure time, expected SOC and so on. After receiving the information, the system starts to calculate the optimal charging period and feedback the calculation results to the user. Users choose whether to accept the results: wait for the charging if they accept, or re-input the relevant information or directly start the disordered charging if they do not accept. Users with orderly charging will get compensation after charging, and users with disordered charging will end directly. Optimization flow is shown in Fig. 4.

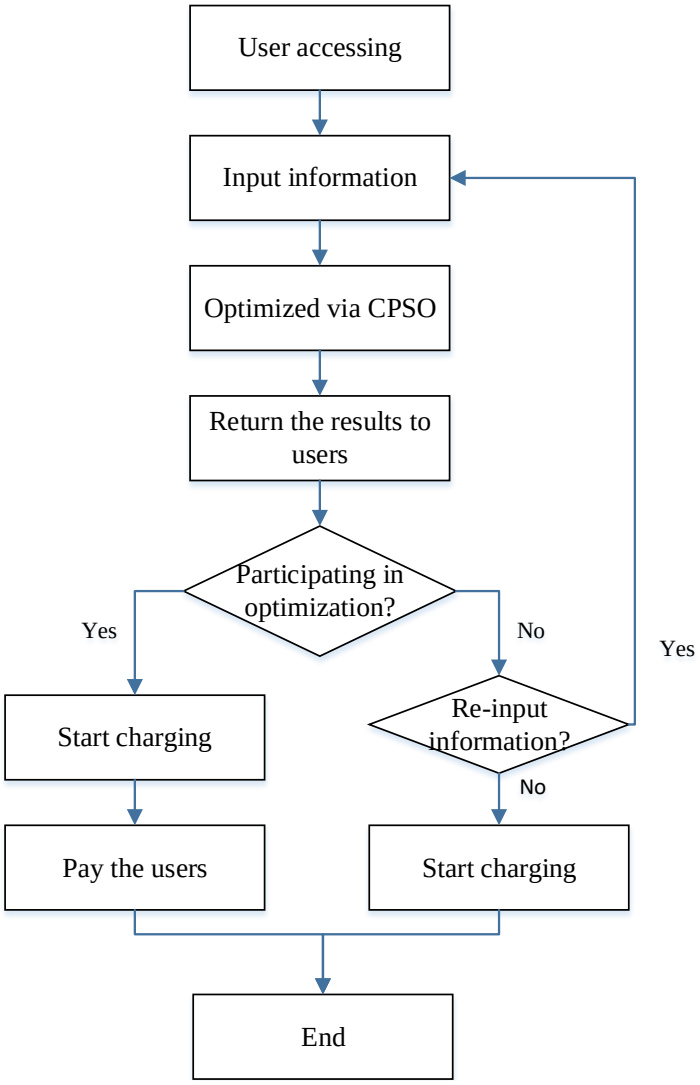

Fig. 4 Charging optimization process

4 Second stage - charging optimization model considering the uncertainty of PV

4.1 Idea of IGDT

The basic idea of IGDT is to reduce the risk caused by uncertainty through a two-stage optimization model. In the first stage, the optimal results expected by the decision-maker is calculated by using the predicted value of uncertain variables. In the second stage, the deviation between the actual value and the predicted value is considered. Decision makers will reserve a certain room for fluctuation, within which the uncertain variables can fluctuate randomly and the decision makers will not suffer economic losses, or even make profits. The IGDT model includes three parts which are basic model, uncertain model, and minimum requirement model [43]. The process of IGDT

modelling is detailed in Fig. 5:

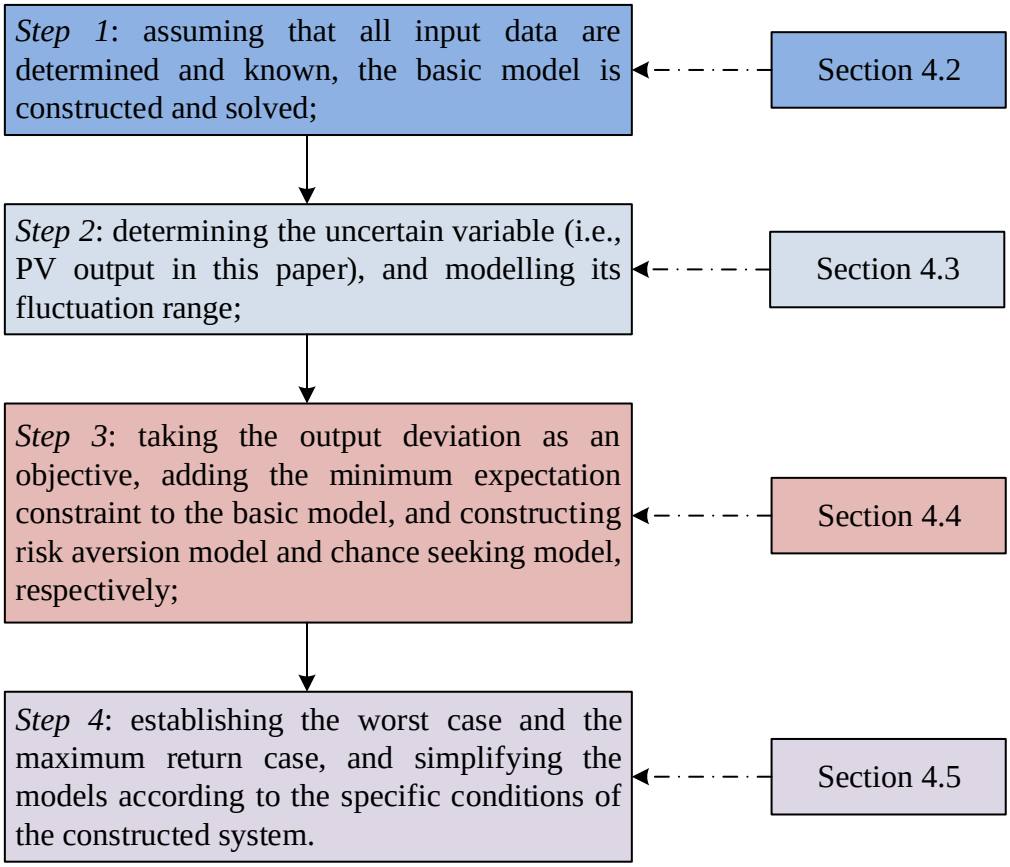

Fig. 5 Steps of IGDT modelling

4.2 Basic model

Basic model refers to the initial optimization model under the assumption that the variables are known and determined (i.e. predicted values), which can be expressed as

$$\begin{cases} \min F\left(u,d\right) \\ s.t. \quad H(u,d)=0 \\ \qquad G(u,d)\le 0 \end{cases} \tag{34}$$

where $F(u,d)$ is the objective function, $H(u,d)$ and $G(u,d)$ are equality and inequality constraints respectively, u is the uncertain variable, and d is the decision variable. The basic model was already detailed in section 3.

4.3 Uncertain variable

u has randomness and volatility, so the predicted value cannot be directly used to represent the actual situation. Its fluctuation can be expressed as:

$$\begin{cases} u \in U(\alpha, \bar{u}) \\ U(\alpha, \bar{u}) = \{u : \left| \dfrac{u - \bar{u}}{\bar{u}} \right| \le \alpha\} \end{cases} \tag{35}$$

where $\bar{u}$ is the predicted value of u, α is the fluctuation range, $\alpha \ge 0$, and $U(\alpha, \bar{u})$ represents that the deviation between u and $\bar{u}$ is not more than $\alpha|u|$.

4.4 Minimum requirement model

When facing uncertainty risks, decision makers may hold different attitudes. One is pessimists who expect to obtain stable returns and fear the loss of benefits caused by risks, and thereby lower expectations to bear risks. The other is optimists who believe that uncertainty may bring greater gains and are willing to take risks to obtain unexpected benefits.

For the former one, robust function is used to resist uncertainty as shown in eq. (36), while for the latter, chance function is applied as presented in eq. (37).

$$\begin{cases} \max \alpha_1 \\ s.t.\ \max\limits_{u} F(u,d) \le (1+\beta_1) F_0 \\ \forall u \in U(\alpha, \bar{u}) \\ H(u,d) = 0 \\ G(u,d) \le 0 \end{cases} \tag{36}$$

$$\begin{cases} \min \alpha_2 \\ s.t.\ \min\limits_{u} F(u,d) \le (1-\beta_2) F_0 \\ \forall u \in U(\alpha, \bar{u}) \\ H(u,d) = 0 \\ G(u,d) \le 0 \end{cases} \tag{37}$$

where F_0 is the optimal value of deterministic model, and $\beta_k, k = 1,2$ is the deviation between actual and predicted values ($k = 1$ is for robust function, while $k = 2$ is for chance function). The robust α_1 can guarantee all objective values of the $F(u,d)$ are not more than $(1+\beta_1)F_0$. The opportunity α_2 can guarantee at least one value of $F(u,d)$ does not exceed $(1-\beta_2)F_0$.

4.5 PV uncertainty modelling based on IGDT

4.5.1 Description of PV uncertainty

The PV output are the uncertain variable in this paper, and the fluctuation is formulated as follows:

$$U(\alpha_{pv},\overline{u_{pv}})=\{u_{pv}:(1-\alpha_{pv})\overline{u_{pv}}\le u_{pv}\le(1+\alpha_{pv})\overline{u_{pv}}\} \tag{38}$$

where α_{pv} is the deviation of PV output, $\overline{u_{pv}}$ is the prediction of PV output, and u_{pv} are the actual output of PV.

4.5.2 Model transformation based on extreme cases

In risk aversion strategy, when the actual output of PV is higher than the predicted, there will be a high penalty cost for energy abandonment. The more the waste energy, the higher the system cost. Therefore, for this strategy, the cost will be the maximum $(1+\beta_1)F_0$ when the PV output reaches the ceiling bound $u_{pv}=(1+\alpha_{pv})\overline{u_{pv}}$. Here, the robust model is transformed to

$$\begin{cases} \max \alpha_{pv} \\ s.t.\ \ (25)-(33) \\ z_1\le(1+\beta_1)F_0 \\ u_{pv,t}=(1+\alpha_{pv})\overline{u_{pv,t}} \\ 0\le\alpha_{pv},\ \ \beta_1\le 1 \end{cases} \tag{39}$$

where z_1 is the objective result considering the uncertain variable. On the contrary, for the opportunity seeking strategy, the model is transformed into

$$\begin{cases} \min \alpha_{pv} \\ s.t.\ \ (25)-(33) \\ z_2\le(1-\beta_2)F_0 \\ u_{pv,t}=(1-\alpha_{pv})\overline{u_{pv,t}} \\ 0\le\alpha_{pv},\ \ \beta_2\le 1 \end{cases} \tag{40}$$

where z_2 is the objective result considering the uncertain variable.

5 Third stage - Shapley-based benefit allocation for the charging system

5.1 Introduction of Shapley method

The Shapley method is selected to distribute the benefits of PV, CCTP, and users, so as to ensure the reasonable benefits of the participants. This method can reflect the overall contribution of the alliance participants and the importance of the participants in the alliance, and avoid the unfairness caused by the average distribution [44]. The model is given by

$$\upsilon_i = \sum_{S \subseteq N} \frac{(|S|-1)!(n-|S|)!}{n!}(v(S)-v(S \setminus i)) \qquad \forall i \in N \tag{41}$$

where υ_i is the allocated benefit of participant i, N is the participant set, $S \setminus i$ is the set of remaining entities except participant i.

5.2 Cooperative premise and mode analysis

The establishment of the alliance needs to meet the following assumptions:

(1) The cost saving of the alliance is more than the sum of individuals' when they are running independently, and then the cooperative alliance can be established;

(2) Considering cleaner production, PV is preferred to power supply;

(3) Considering the uncertainty of PV, thermal power is required to provide a backup.

Therefore, **cooperative mode** includes:

(1) **Independent operation:** users charge disorderly, PV provides its own power generation and purchases electricity from public grid to meet the demands;

(2) **PV-CCTP:** PV has priority to supply power, and the CCTP meets the remaining demands;

(3) **PV-users:** users charge in order, and PV gives compensation to the users for participation;

(4) **PV-CCTP-users:** users orderly charge, PV supplies power first, and CCTP meets the remaining demands as a backup.

5.3 Cost calculation model in different cooperation alliances

5.3.1 Independent operation case

(1) PV

In this case, the total cost of PV contains power generation cost c_{pg}^{pv}, power purchase cost c_{ep}^{pv}, energy abandonment penalty c_{fine}^{pv}, and CO_2 emission cost $c_{emission}^{pv}$, i.e.,

$$c_{pv} = c_{pg}^{pv} + c_{ep}^{pv} + c_{fine}^{pv} + c_{emission}^{pv} \tag{42}$$

(2) CCTP

In this case, CCTP is not included, so the cost of it is $c_{tu} = 0$.

(3) Users

Users charge disorderly, so the cost of users only includes charging cost.

5.3.2 PV-CCTP cooperation case

(1) PV

In this case, the unmet load is satisfied by the CCTP, so the PV no longer pay the power purchase cost, i.e.,

$$c_{pv} = c_{pg}^{pv} + c_{fine}^{pv} + c_{emission}^{pv} \tag{43}$$

(2) CCTP

CCTP is considered in this case, so the cost of it is given by

$$c_{tu} = c_{pg}^{tu} + c_{cs}^{tu} + c_{ce}^{tu} - r_{ce}^{tu} \tag{44}$$

where c_{pg}^{tu}, c_{cs}^{tu}, c_{ce}^{tu}, and r_{ce}^{tu} are the costs for fuel, carbon storage, and emissions, and income from carbon trades.

(3) Users

The cost of users only includes charging cost.

5.3.3 PV-users cooperation case

(1) PV

In this case, PV needs to pay compensation c_{pro}^{pv} to users to encourage them to actively participate in optimization, and still, power purchase cost exists, i.e.,

$$c_{pv} = c_{pg}^{pv} + c_{pro}^{pv} + c_{ep}^{pv} + c_{fine}^{pv} + c_{emission}^{pv} \tag{45}$$

(2) CCTP

The total cost of CCTP is 0.

(3) Users

Users participating in optimization gain a profit I_{pro}^{user}, so the cost is given by

$$c_{user} = c_{cha}^{user} - I_{pro}^{user} \tag{46}$$

5.3.4 PV-CCTP-users cooperation case

(1) PV

In this case, power purchase is not needed, but compensation for users is generated, i.e.,

$$c_{pv} = c_{pg}^{pv} + c_{pro}^{pv} + c_{emission}^{pv} + c_{fine}^{pv} \tag{47}$$

(2) CCTP

The cost is similar to the model in subsection 5.3.2

(3) Users

The cost is similar to the model in subsection 5.3.3.

6 Example analysis

6.1 Addressing load uncertainty

6.1.1 Markov Chain based quantity prediction of EVs

Travel data of cars in the NHTS 2017 database were selected [45], and the model of BYD e6 was selected as shown in Table 1 [12]. The SOC between [10%,85%] of EVs in the three areas were selected to calculate the transfer probability matrix. Assuming that the original numbers in H, W, and O were $N_0 = [800, 200, 300]$. The calculation process is shown in eq. (48), and the number curves of H and W are depicted in Fig. 6. With 5% confidence, the value of chi-square was located between $\chi^2 \in [9.68, 847.15]$, meeting the requirement of exceeding 9.49.

Table 1 Basic parameters

Parameter	Explanation	Value
E_{bat}	Rated capacity	82 kWh
ε	Driving efficiency	95%
e	Power consumption of EVs travelling per unit	20.5 kWh/100km
P_{char}	Charging power	10 kW

$$\underbrace{\begin{bmatrix} t \backslash t+1 & h & w & o \\ h & 0.4375 & 0.125 & 0.4375 \\ w & 0.8947 & 0.1053 & 0 \\ o & 0.8785 & 0.0055 & 0.1160 \end{bmatrix} \begin{bmatrix} 0.3 & 0.3 & 0.4 \\ 0.85 & 0.05 & 0.1 \\ 0.9109 & 0.0099 & 0.0792 \end{bmatrix} \cdots \begin{bmatrix} 0.4375 & 0.1042 & 0.4583 \\ 0.8965 & 0.0575 & 0.0460 \\ 0.9104 & 0.0022 & 0.0874 \end{bmatrix}}_{P_0 P_1 \cdots P_{23}} \tag{48}$$

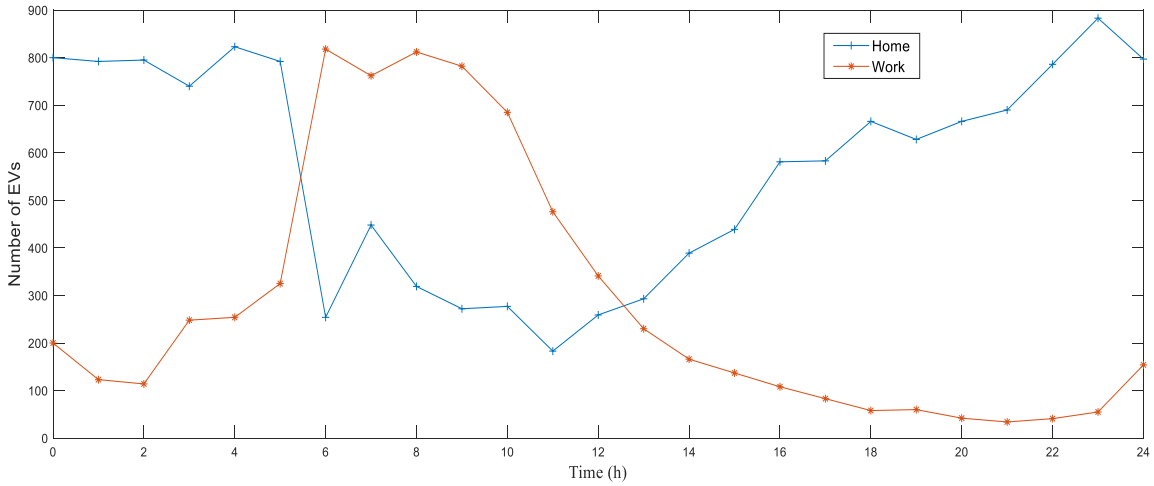

Fig. 6 Numbers of EVs in H and W

6.1.2 Mileage fitting result

The fitting result is shown in Fig. 7, and the parameters of the fitting distribution function were $\mu = 1.2051, \sigma = 1.2766$. The Root Mean Squared Error was 6.729 and R-square was 0.9878, which are better than the result of [12].

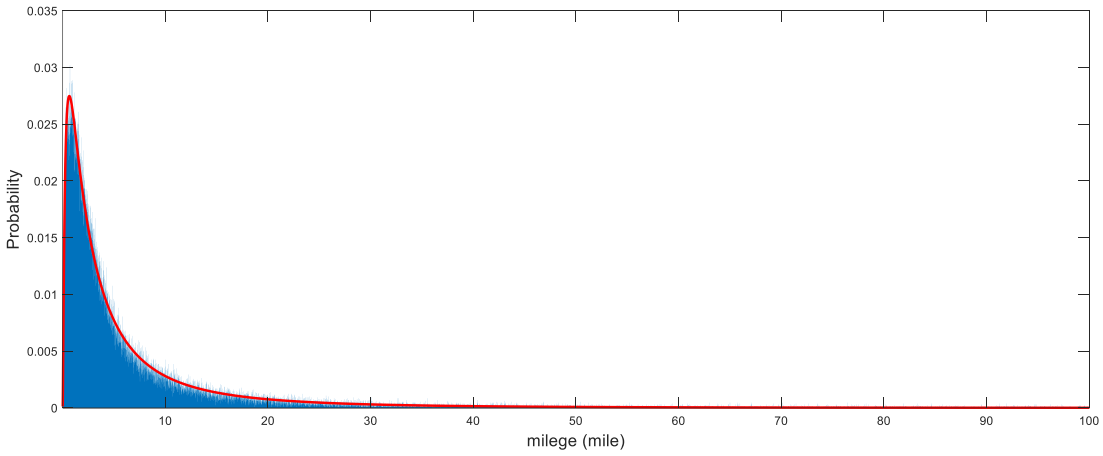

Fig. 7 Mileage fitting results

6.1.3 Charging load result

Different from the work of [12], we also fitted the speed distribution. Based on NHTS2017 database, the travel data of EVs within the safe stored range [10%, 85%] set in this paper were selected, and the fitting results were $\mu = 3.2651, \sigma = 0.9792$. Then, the data of mileages and speeds are generated. Finally, the charging load curves are depicted in Fig. 8.

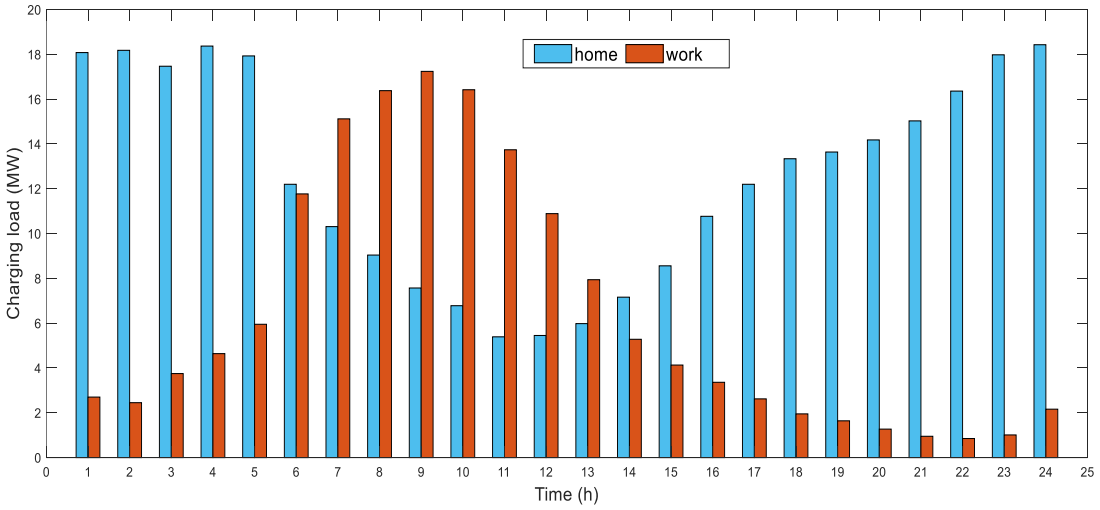

Fig. 8 Charging loads in home and work areas

According to Fig. 6, the load in H was mostly distributed at night and in early morning. From 6:00 on, the charging load gradually decreased due to users going to work. After reaching the low point at 11:00, it gradually increased. The change trend in W was just the opposite: the load increased gradually after 6:00, reached the peak at 9:00, and the charging peak period is from 5:00 to 11:00, which is just the commuting time of users; the load decreased gradually after 13:00, and the load was the lowest at night. The results show that the peak and valley of charging load in H and W were staggered, which is in line with the actual situation.

6.2 Orderly charging optimization analysis

6.2.1 Basic data

PV output is detailed in the work of [3], and the charging loads in H and W are shown in subsection 6.1. The power generation cost per unit of PV is set to be 600 ￥/MWh[3]. According to the works of [4, 46, 47], for CCTP, the operation energy consumption for addressing a unit of CO_2 is set to be 0.23 MW·h/tCO_2, CO_2 emission quota for a unit of power generation is set to be 0.76 t/(MW·h), the fixed power consumption is 3MW, CO_2 capturing rate is 0.9, carbon storage cost is 31.8 ￥/t, carbon trading price is set to be 126.5 ￥/tCO_2, CO_2 emission intensity per unit of power generation is 0.96t/MWh, fuel cost coefficients a, b and c are set to be 0.133, 126.5, and 2188, and energy curtailment penalty is set to be 200 ￥/MWh. Users participating in optimization can get a price discount of 20%, and power purchase cost of PV is set to be 1.2 times of the cost of the traditional thermal power.

The time division was obtained as shown in Table 2, along with the corresponding price.

Table 2 Time division and TOU price

Period	Duration for	Duration for	Price

division	work place	home area	(￥/MWh)
Peak	5：00-11：00	0:00-5:00 22:00-24:00	1753.7
Flat	11：00-17：00	5:00-9:00 and 15:00- 22:00	1442.4
Valley	0：00-5：00, 17：00-24：00	9:00-15:00	1140.8

6.2.2 Verifying the superiority of the proposed charging system

We set up two cases (as shown in Table 3) to verify the superiority of the proposed system. Therein, in Case 1-1 PV cooperates with traditional thermal power while both PV and CCTP supply power to users in Case 1-2.

Table 3 Case setup

Case	Alliance	Ordered charge	PV uncertainty
Case 1-1	PV and traditional thermal power	×	×
Case 1-2	PV and CCTP	×	×

We used the charging load in W area to verify the superiority. Figure 9 shows the differences of the total cost of the system, and Table 4 shows some indicators that had a change.

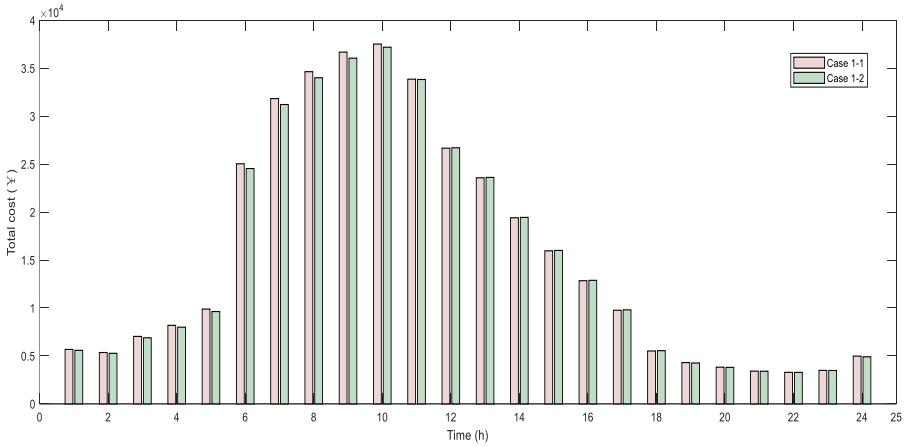

Fig. 9 Cost comparison between two cases at each time point

Table 4 Result-changed indicators

Case	Fuel cost of thermal power(￥)	Carbon storage cost (￥)	Carbon trading income (￥)	Gross power generation cost (￥)	CO_2 emission (t)
Case 1-1	63747.00	-	-	130912.14	84.432
Case 1-2	67535.98	2416.44	7387.45	127504.98	8.443

According to Fig. 7, the total cost in Case 1-2 basically was lower than that in Case 1-1. According to Table 4, although traditional thermal power did not have carbon storage cost, it did not gain carbon trading income, either; and CO_2 emissions were

higher than CCTP. The process of CCS made the CCTP cost more fuel and generate carbon storage cost, but the carbon trading income made up for it and the emission cost was reduced, and thus the total cost in Case 1-2 was lower than that in Case 1-1 by ￥3407.16. Therefore, the superiority of the proposed system was verified.

6.2.3 Verifying the effectiveness of the optimization model

We set up 6 cases (as shown in Table 5) to discuss the charging optimization results. Alliance forms of Cases 2-1 to 2-4 has discussed in subsection 5.2, we will not go into details here. Based on Case 2-4, uncertainty of PV is considered in cases 2-5 and 2-6 where case 2-5 is set up for risk averter and case 2-6 is for opportunity seeker. The acceptable cost change is set to be 10%.

Table 5 Case setup

Case	Alliance	PV	CCTP	Ordered charge	Uncertainty of PV	
					Risk aversion	Opportunity pursuit
Case 2-1	No cooperation	√	×	×	×	×
Case 2-2	PV-CCTP	√	√	×	×	×
Case 2-3	PV-users	√	×	√	×	×
Case 2-4	PV-CCTP-users	√	√	√	×	×
Case 2-5	PV-CCTP-users	√	√	√	√	×
Case 2-6	PV-CCTP-users	√	√	√	×	√

The results are analyzed as follows.

(1) Comparison in terms of load curve change

In Case 2-3, users participate in the optimization. Figure 10 compares the charging load curves before and after the optimization and the matching degrees with PV output. Table 7 presents some calculation results.

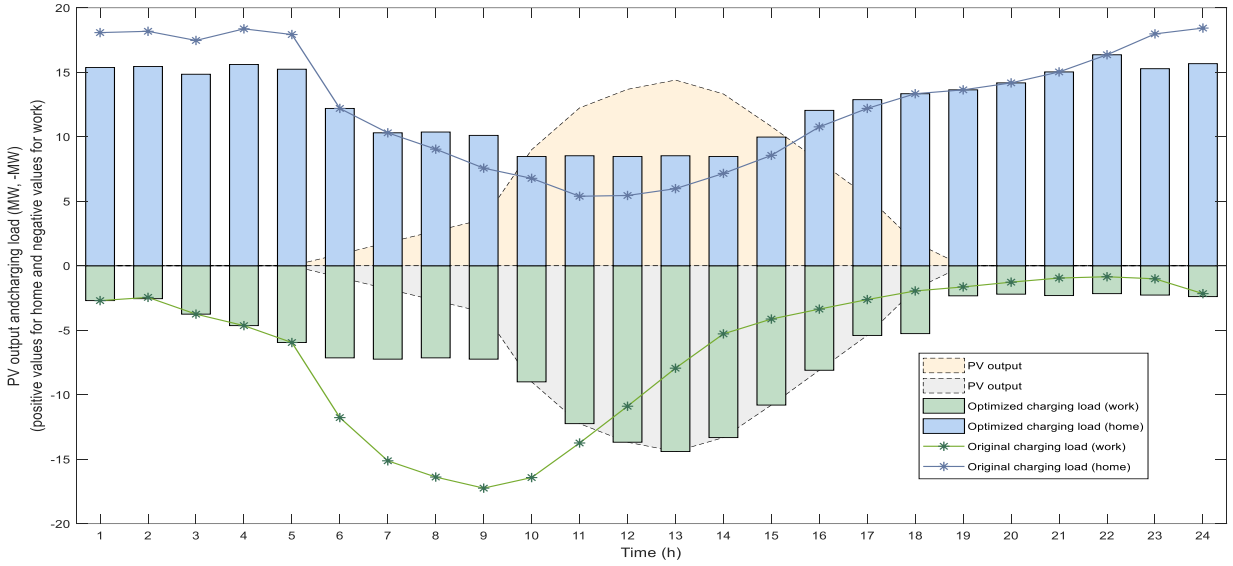

Fig. 10 Optimization results

In the working area, the charging peak of users here was mainly in the morning

working hours, and users usually started charging after arriving, so the charging peak was 5:00-11:00; while the peak of PV was after 10:00. Obviously, the load and power generation did not match: the average source-load deviation was 4.98 MW, and the maximum deviation was 18.43MW (which occurred at 8:00). Most users could transfer the charging time to the peak period of PV output, because of their staying in the working area during this period, so as to reduce energy abandonment and output of thermal power. After the orderly charging optimization, the average deviation of source and load decreased by 52.72%, the maximum deviation decreased by 54.39%, and the load fluctuation decreased by 49.82%.

In the home area, the peak charging time was at night, and yet it was the valley time of PV power generation. Since most users charge for the next day's commuting, relatively few users could participate in the optimization, so even through the optimization, there was still energy abandonment during the generation peak of PV. After optimizing, the average deviation decreased by 9.72%, the maximum deviation decreased by 11.23%, and the load fluctuation decreased by 63.40%.

(2) Comparison in terms of energy usage

Outputs in different cases are presented in Figs. 11 and 12. PV curtailment is shown in Table 6.

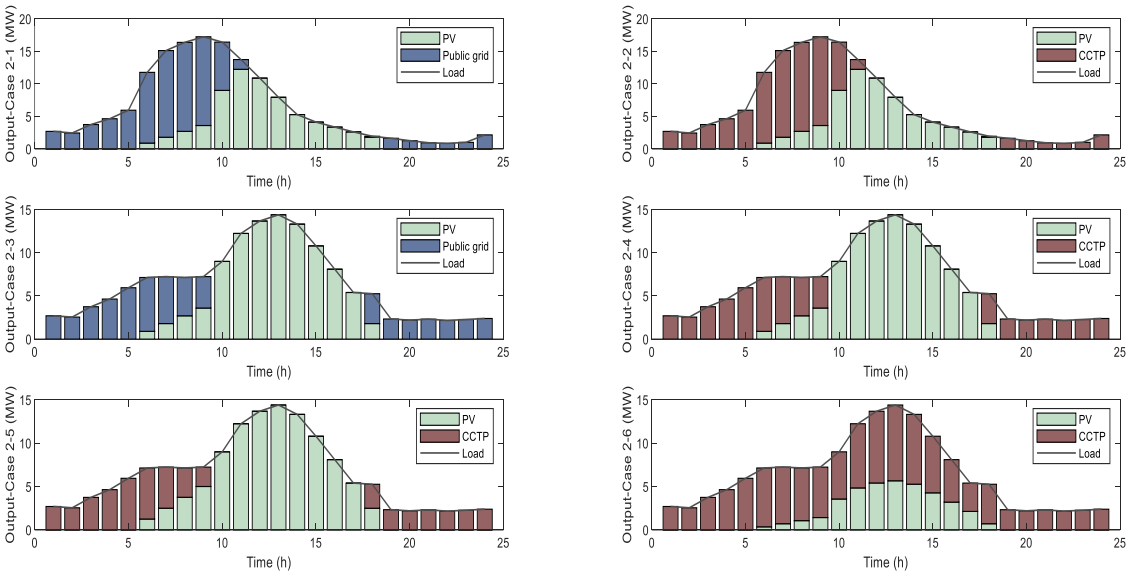

Fig. 11 Outputs of working area

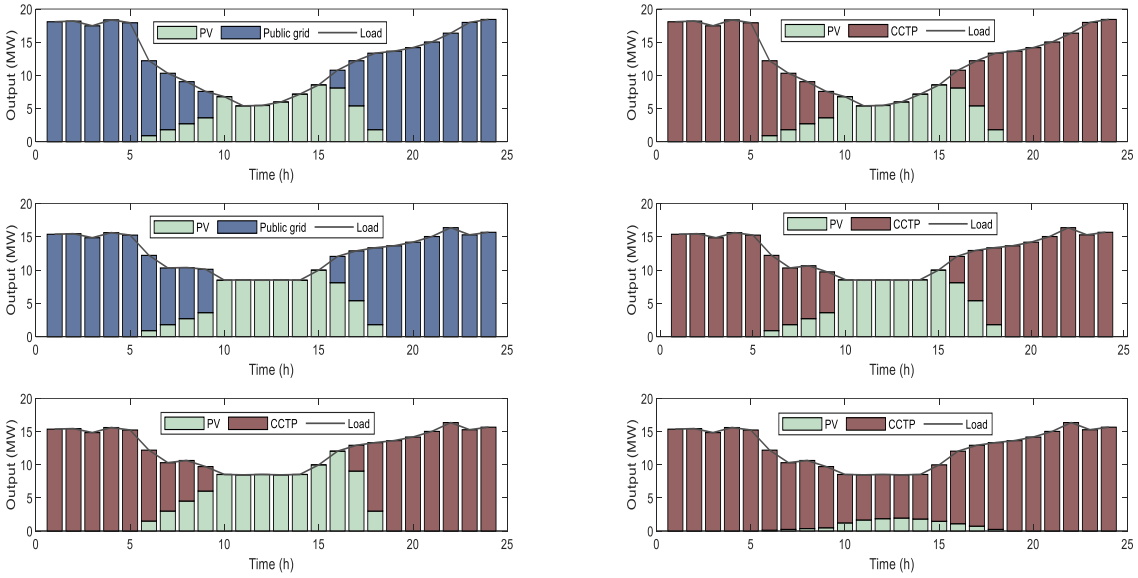

Fig. 12 Outputs of home area

Table 6 PV curtailment (Unit: MW)

Work					
Case 2-1	Case 2-2	Case 2-3	Case 2-4	Case 2-5	Case 2-6
31.48	31.48	0	0	34.11	0
Home					
Case 2-1	Case 2-2	Case 2-3	Case 2-4	Case 2-5	Case 2-6
34.12	34.12	20.98	20.98	71.98	0

Comparing different areas, we can see that the matching degree of working area was higher than that of home area, and the users had stronger willingness to cooperate, so the PV utilization performance of the working area in each case was better. Moreover, it can be noted that the more factors we considered, the greater the gap in the performance of PV utilization between the two areas. With the employment of CCTP, the participation of users for ordered charge, and the consideration of negative effect of PV's uncertainty, the differences of energy curtailment between the two areas were 2.64 MW, 20.98 MW, and 37.87 MW, respectively.

Comparing different cases, we can see that in the deterministic optimization model, PV curtailment was greatly reduced when users charged in peak time of PV output. Compared with the cases where users did not participate in the optimization, ordered charge in working area made the PV generation completely consumed, and the abandoned energy was reduced by 38.51%. Due to the deviation of PV output in the IGDT-based model, there were two possible changes of the abandoned energy. In the risk aversion strategy, the increase of PV output led to more risks, so the abandoned energy was increased by 2.63 MW (work) and 37.86 MW (home) compared with the user non-cooperation cases, and it was also increased by 34.11MW (work) and 51MW (home) compared with the user cooperation cases. In the opportunity seeking strategy, PV generation is less than the predicted, so the two areas can consume all the energy.

(3) Comparison in terms of CO_2 emission

Table 7 CO_2 emission (Unit: ton)

Work					
Case 2-1	Case 2-2	Case 2-3	Case 2-4	Case 2-5	Case 2-6
84.432	8.443	54.211	5.421	5.016	11.096
Home					
Case 2-1	Case 2-2	Case 2-3	Case 2-4	Case 2-5	Case 2-6
227.309	22.731	214.697	21.464	20.036	27.562

In terms of environmental benefits, we can see from Table 7 that the CCS can greatly reduce CO_2 emissions. In comparison of Cases 2-1 and 2-2, the CO_2 emissions in the CCTP involved case greatly reduced by 90.00% (work) and 35.79% (home). In Case 2-5, the increase of PV output made less power of CCTP (decreased by 7.47% (work) and 6.65% (home)), but it made the energy abandonment issue more serious. In Case 2-6, the reduction of PV output required the system to have more needs of thermal power output, so the CO_2 emission was increased by 104.69% (work) and 28.41% (home), compared with Case 2-4.

(4) Comparison in terms of economic benefits

Table 8 Cost comparison

Area	Case	Cost of PV (¥)	Fuel cost of thermal power (¥)	CO_2 storage cost (¥)	Carbon trading income (¥)	Cost of CCTP (¥)	Charging cost of users (¥)	Total cost of the system (¥)
Work	Case 2-1	144106.56	63747.00	-	-	-	241815.16	385921.73
	Case 2-2	64940	67535.98	2416.44	7387.45	62564.98	241815.16	369320.14
	Case 2-3	143159.73	59685.96	-	-	-	164744.63	307904.35
	Case 2-4	69822.14	62440.10	1551.52	4743.25	59248.37	164744.63	293815.14
	Case 2-5	99638.75	61766.69	1435.57	4388.77	58813.49	164744.63	323196.87
	Case 2-6	34352.05	71869.88	3175.77	9708.83	65336.82	164744.63	264433.50
Home	Case 2-1	172190.04	82944.50	-	-	-	460798.82	632988.86
	Case 2-2	65468	91624.81	6505.58	19888.57	78241.81	460798.82	604508.63
	Case 2-3	167078.32	81206.72	-	-	-	338017.47	505095.79
	Case 2-4	67503.71	89421.75	6142.97	18780.03	76784.69	338021.09	482309.49
	Case 2-5	117276.71	87037.95	5734.35	17530.81	75241.48	338021.09	530539.28
	Case 2-6	12650.82	99597.33	7888.33	24115.87	83369.79	338021.09	434041.69

In the case of non-cooperation, in addition to the power generation cost, PV also needed to pay high power purchase cost to meet the demand of charging load, which burdened PV and also increased the total cost of the system.

In the PV-CCTP cooperation case, PV no longer paid for the power purchase, and CCTP met the residual charging demand instead. Therefore, PV cost less. Although addressing CO_2 required energy consumption and carbon storage cost, CO_2 emission cost decreased and carbon trading income deducted some cost, and thereby the total cost of the system was lower than that of Case 2-1 by 4.30% (work) and 4.50% (home).

In the PV-users cooperation case, users were encouraged to charge in PV generation peak hours by giving them some compensations. Although the compensation increased the cost of PV, the punishment for abandoning energy and the power purchase cost were reduced. It turned out that the total cost of the system was reduced by 16.63% (work) and 16.45% (home), compared with Case 2-2.

In the PV-CCTP-users cooperation case, CCTP replaced public grid for power supplement, and its total cost was much smaller than the power purchase cost, so the total cost of the system was further reduced, which was lower than that of Case 2-3 by

4.58% (work) and 4.51% (home).

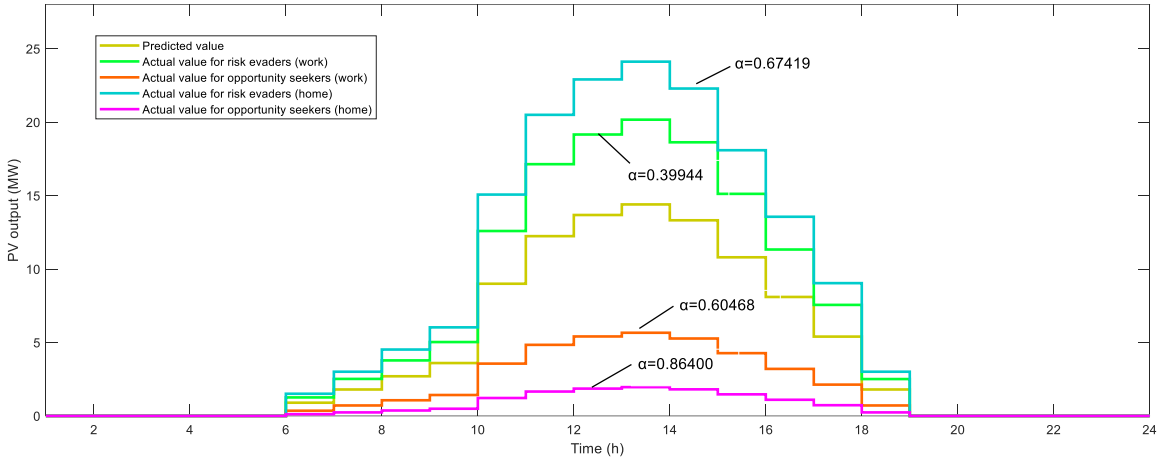

Fig. 13 Changes of PV output

Changes of PV output in the two strategies are shown in Fig. 13. In risk aversion strategy, when the increases of PV output were in the ranges of [0,39.944%] (work) and [0,67.419%] (home), the deviations of cost fluctuating within [0, ¥29381.21] (work) and [0, ¥48229.79] (home) were acceptable for pessimistic decision makers, which reflected the robustness of IGDT model. In opportunity seeking strategy, when the PV reductions fluctuated within the ranges of [0,60.468%] (work) and [0,86.400%] (home), optimistic decision makers can reduced the cost by [0, ¥29381.21] (work) and [0, ¥96497.59] (home), which reflected the opportunism of IGDT model.

(5) Sensitivity analysis based on different acceptable level of cost fluctuation

Change trajectories of uncertainty coefficient and acceptable cost are shown in Fig. 14.

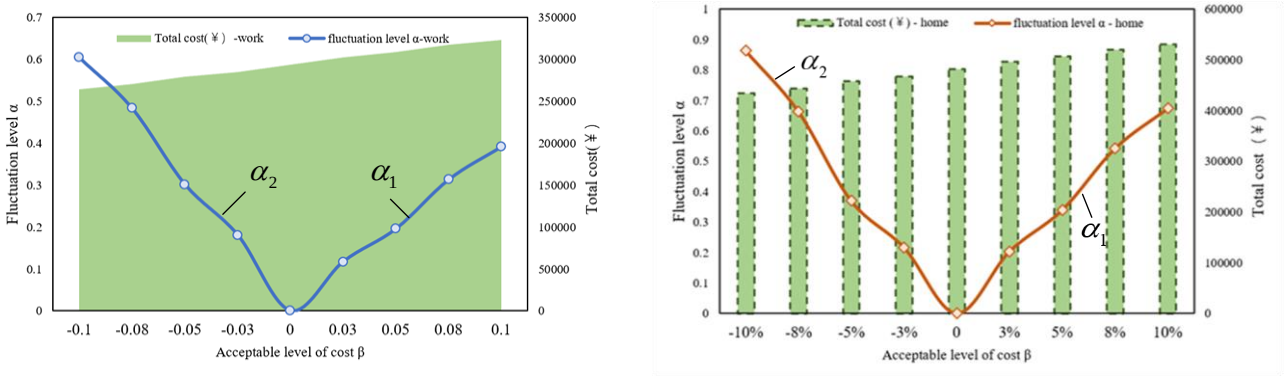

Fig. 14 Change trajectories of uncertainty coefficient and acceptable cost

As shown in Fig. 14, when acceptable cost increased, α_1 (the robust alpha) and α_2 (the opportunity alpha) showed an increase and a decrease, respectively.

For α_1, the larger the value, the more pessimistic the decision-maker's view on photovoltaic fluctuation, the more afraid of the energy abandonment penalty brought by the more power generation of PV than predicted, and the higher the robustness of the system. A smaller value of α_2 means that the decision-maker's optimism about the

additional benefits generated by PV output fluctuations was reduced and the cost was also increased.

6.3 Benefit allocation results

6.3.1 Economic benefit allocation

Based on the optimal deterministic case, risk aversion and opportunity pursuit cases, cost-saving benefits are distributed, respectively. the cost savings are shown in Table 9 (the cost savings of alliances and non-cooperation which are not mentioned in the table are 0), and allocation results are shown in Table 10.

Table 9 Cost savings (¥)

Area	Uncertainty of PV	PV-CCTP	PV-users	PV-CCTP-users
Work	Deterministic	16601.59	78017.37	92106.59
	Risk aversion	15894.98	76269.05	90582.53
	Opportunity seeking	18825.61	66032.39	84871.73
Home	Deterministic	28480.23	127893.1	150679.4
	Risk aversion	27389.47	128386.2	149979.7
	Opportunity seeking	32519.05	122841	150698.8

Table 10 Allocation results

Area	Entity	Case 2-4 based (¥)	Case 2-5 based (¥)	Case 2-6 based (¥)
Work	PV	46472.02	45554.85	42433.58
	CCTP	7463.34	7420.33	9417.38
	users	38171.23	37607.36	33020.77
Home	PV	76288.67	75955.86	76126.28
	CCTP	12342.14	11762.76	14705.80
	users	62048.56	62261.13	59866.76

According to Table 10, as the main power supplier, PV could obtain the largest share of system benefits, accounting for 50% of the total cost savings. The user's adjustment of charging plan could not only reduce the PV energy abandonment, but also reduce the cost of CCTP, so it ranked second in terms of contribution, and obtained about 40% cost saving shares. Although the CCTP could significantly reduce CO_2 emissions, its power generation cost was still higher than the unit cost of PV. Compared with the other two main bodies, its contribution was relatively small, obtaining about 10% of the total cost savings.

6.3.2 Comprehensive benefit allocation

Benefit allocation from economic perspective does not consider the environmental contribution of CCTP since it is an important means for reducing CO_2 emissions. Therefore, we reallocated the benefits both economically and environmentally, and the results were normalized and are shown in Table 11.

Table 11 Low-carbon and economic-based benefit allocation results

Area	Entity	Case 2-4 based	Case 2-5 based	Case 2-6 based	Proportion of average benefit
Work	PV	0.243	0.244	0.250	52.35%
	CCTP	0.098	0.100	0.153	24.93%
	users	0.104	0.119	0.097	22.71%
Home	PV	0.248	0.248	0.249	50.63%
	CCTP	0.137	0.134	0.149	28.51%
	users	0.104	0.105	0.098	20.86%

According to Table 11, PV had obvious advantages in economic and environmental benefits, so it still obtains the largest benefit distribution proportion, which is basically consistent with the original distribution result. In terms of reducing CO_2 emissions, the capacity of CCTP was much greater than the contribution made by users to the system. In addition, limited by the source-load matching degree and responsiveness to the optimization, users will no longer contribute to the system after the PV output was completely consumed. Therefore, the benefits of CCTP was significantly increased while the user's was reduced. The final allocation results are more reasonable.

Above all, for the proposed charging system, the decision maker should focus on the consumption of PV. On the one hand, a more positively incentive scheme should be considered to encourage more users to charge during the peak period of PV output and smooth the charging load curve. On the other hand, the CCTP should be employed to reduce CO_2 emissions and to develop interaction with the carbon trading market, so as to maximize the benefits and achieve a win-win situation in the power generation and consumption sides.

7 Conclusions

In this paper, a three-stage model is proposed to optimize the EV charge and distribute the benefits. In the first stage, Markov chain and Monte Carlo are used to obtain the charging loads of work area and home area, and the deterministic charging optimization model is established with the objectives of economic, environmental-friendly, and energy utilization-based benefits and load fluctuation. In the second stage, uncertainty of PV is introduced, and the IGDT based optimization model is constructed by maximizing / minimizing photovoltaic deviations, and two strategies, i.e., risk aversion and opportunity pursuit are proposed. In the third stage, based on Shapley method, benefits are allocated for the optimal cases, i.e., the deterministic one, risk

aversion and opportunity pursuit. The results show that:

(1) The proposed method for addressing charging load uncertainty with the consideration of quantity transfer and vehicle speed differences can effectively depict the charging load curve.

(2) Employing carbon capture and storage system can effectively reduce the CO_2 emissions of the system, and make up for the cost through obtaining carbon trading income; such joint system reduces the emission by 85.08% and the cost by 2.60%.

(3) PV-CCTP-users cooperative alliance makes 3E benefits maximum, and also makes load curve smoother; the cost is decreased by at least 4.51%, emissions are reduced by at least 4.59%, PV consumption is increased by 38.51%, and the load fluctuation is reduced by at least 49.82%.

(4) When the exact probability distribution cannot be obtained, the IGDT model can effectively address the uncertainty of photovoltaics to obtain the robust solution and the opportunistic solution. No matter how the uncertain variables change, the risk aversion strategy can ensure that the final optimization result is within the expected range; The opportunity pursuit strategy provides the lowest income threshold reference for decision makers who dare to take risks. Both of the strategies can quantitatively describe the relationship between the variation range of uncertainty and the minimum acceptable goal, and thus provide differentiated solutions for decision makers with different preferences.

(5) Economically, the benefit allocation ratio of PV-CCTP-users is about 5:1:4, which reflects the economy of photovoltaic power generation and order charge, but it ignores the environmental contribution of CCTP; After considering the emission reduction factor, the result is about 5:3:2, which indicates the significant contribution of carbon capture thermal power to emission reduction. Thus, the multi-dimensional benefit allocation is more reasonable.

Funding

This research was funded by The National Key R&D Program of China, grant number 2020YFB1707801, and the China Scholarship Council Joint Ph.D. Program, grant number CSC202206730084.

Reference

[1] Derrick Kwadwo Danso BF, Benoit Hingray, Arona Diehiou. Assessing hydropower flexibility for integrating solar and wind energy in West Africa using dynamic programming and sensitivity analysis. Illustration with the Akosombo reservoir, Ghana. Journal of Cleaner Production. 2021;287.

[2] Ashkan Toopshekan HY, Fatemeh Razi Astaraei. Technical, economic, and performance analysis of a hybrid energy system using a novel dispatch strategy. Energy. 2020;213.

[3] LIN Hongyu YQ, DE Gejirifu, YANG Shenbo, WU Jing, FAN Wei, TAN Zhongfu, CUI Zhantao. Peak-Regulation Optimization Model for Gas-Fired Generators in Parks with P2G Employed Under Mixed Market Environment. Electric Power Construction. 2020;41:106-15.

[4] ZHONG Wuzhi HS, CUI Yang, XU Jiakai, ZHAO Yuting. W-S-C Capture Coordination in Virtual Power Plant Considering Source-load Uncertainty. Power System Technology. 2020;44:3424-32.
[5] QU Fumin ZJ, CAI Zhi, HU Chaofan, DAI Sai, SUN Qian. Coordinated Optimal Control Strategy for Electric Vehicle and Thermostatically- controlled Load Aggregators. Proceedings of the CSU-EPSA. 2021;33:48-56.
[6] Zhou Hu XL. A novel Markov chain method for predicting granular mixing process in rotary drums under different rotation speeds. Powder Technology. 2021;386:40-50.
[7] TIAN Mengyao TB, YANG Xiu, XIA Xiangwu. Planning of Electric Vehicle Charging Stations Considering Charging Demands and Acceptance Capacity of Distribution Network. Power System Technology. 2021;45:498-509.
[8] LV Lin XW, XIANG Yue, ZHANG Yi, XIONG Jun. Optimal Allocation of Charging Piles in Multi-areas Considering Charging Load Forecasting Based on Markov Chain. ADVANCED ENGINEERING SCIENCES. 2017;49:170-8.
[9] XU Wei LL, XU Lixiong, XIANG Yue. Calculation of Charging Demand from Electric Vehicles Based on Markov Chain. Proceedings of the CSU-EPSA. 2017;29:12-9.
[10] SHU Jun TG, HAN Bing. Two-Stage Method for Optimal Planning of Electric Vehicle Charging Station. Transactions of China Electrotechnical Society. 2017;32:10-7.
[11] Yan Jie ZJ, Liu Yongqian, Lv Guoliang, Han Shuang, Alfonzo Ian Emmanuel Gonzalez. EV charging load simulation and forecasting considering traffic jam and weather to support the integration of renewables and EVs. RENEWABLE ENERGY. 2020;159:623-41.
[12] Han Xiaojuan WZ, Hong Zhenpeng, Zhao Song. Ordered charge control considering the uncertainty of charging load of electric vehicles based on Markov chain. RENEWABLE ENERGY. 2020;161:419-34.
[13] Borray AFC GA, Merino J, Torres E, Mazon J. New energy bound-based model for optimal charging of electric vehicles with solar photovoltaic considering low-voltage network's constraints. INTERNATIONAL JOURNAL OF ELECTRICAL POWER & ENERGY SYSTEMS. 2021;129.
[14] Climent Hector PB, Bares Pau, Pandey Varun. Exploiting driving history for optimising the Energy Management in plug-in Hybrid Electric Vehicles. ENERGY CONVERSION AND MANAGEMENT. 2021;234.
[15] Da silva Samuel Filgueira EJJ, Silva Fabricio Leonardo, Silva Ludmila C.A., Dedini Franco Giuseppe. Multi-objective optimization design and control of plug-in hybrid electric vehicle powertrain for minimization of energy consumption, exhaust emissions and battery degradation. ENERGY CONVERSION AND MANAGEMENT. 2021;234.
[16] Jony Javorski Eckert SFdS, Maria Augusta de Menezes Lourenco, Fernanda Cristina Correa, Ludmila C.A. Silva, Franco Giuseppe Dedini. Energy management and gear shifting control for a hybridized vehicle to minimize gas emissions, energy consumption and battery aging. ENERGY CONVERSION AND MANAGEMENT. 2021;240.
[17] Zheng Yanchong SZ, jian Linni. The peak load shaving assessment of developing a user-oriented vehicle-to-grid scheme with multiple operation modes: The case study of Shenzhen, China. SUSTAINABLE CITIES AND SOCIETY. 2021;67.
[18] Yuna Wu HX, Chuanbo Xu, Kaifeng Chen. Uncertain multi-attributes decision making method based on interval number with probability distribution weighted operators and stochastic dominance degree. Knowledge-Based Systems. 2016;113:199-209.
[19] Shenbo Yang ZT, Zhixiong Liu, Hongyu Lin, Liwei Ju, Fengao Zhou, Jiayu Li. A multi-objective

stochastic optimization model for electricity retailers with energy storage system considering uncertainty and demand response. Journal of Cleaner Production. 2020;277.
[20] Zhongfu Tan WF, Hanfang Li, Gejirifu De, Jiale Ma, Shenbo Yang, Liwei Ju, Qingkun Tan. Dispatching optimization model of gas-electricity virtual power plant considering uncertainty based on robust stochastic optimization theory. Journal of Cleaner Production. 2020;247.
[21] Erfan Babaee Tirkolaee AM, Zahra Dashtian, Mehdi Soltani, Gerhard-Wilhelm Weber. A novel hybrid method using fuzzy decision making and multi-objective programming for sustainable-reliable supplier selection in two-echelon supply chain design. Journal of Cleaner Production. 2020;250.
[22] Yue Yin TL, Chuan He. Day-ahead stochastic coordinated scheduling for thermal-hydro-wind-photovoltaic systems. Energy. 2019;187.
[23] WEI Zhenbo GY, WEI Ping'an, HUANG Yuhan. An IGDT based Multi-objevtive Expansion Planning Model for Integrated Natural Gas and Electric Power Systems. High Voltage Engineering. 2021.
[24] PAN Zhaoming LS, WANG Zhijie, WANG Shuai, DING Chaoran. Dispatch Based on Information Gap Decision Theory for Power System with Wind Power. Electric Power Construction. 2018;39:87-94.
[25] Najafi A, Pourakbari-Kasmaei, M., Jasinski, M., Lehtonen, M., & Leonowicz, Z. A medium-term hybrid IGDT-Robust optimization model for optimal self scheduling of multi-carrier energy systems. Energy. 2022;238.
[26] Morteza Shafiekhani AA, Omid Homaee, Miadreza Shafie-khah, Joao P.S., Catalao. Optimal bidding strategy of a renewable-based virtual power plant including wind and solar units and dispatchable loads. Energy. 2022;239.
[27] Chen Qixin KC, Xia Qing. Operation mechanism and peak-load shaving effects of carbon-capture power plant. Proceedings of the CSEE. 2010;30:22-8.
[28] Xingping Zhang YZ. Environment-friendly and economical scheduling optimization for integrated energy system considering power-to-gas technology and carbon capture power plant. Journal of Cleaner Production. 2020;276.
[29] Taljegard M. GL, Odenberger M., Johnsson F. Impacts of electric vehicles on the electricity generation portfolio - A Scandinavian-German case study. APPLIED ENERGY. 2019;235.
[30] Cao Zhiao WJ, Zhao Qiang, Han Yinghua, Li Yuchun. Decarbonization Scheduling Strategy Optimization for Electricity-Gas System Considering Electric Vehicles and Refined Operation Model of Power-to-Gas. IEEE ACCESS. 2021;9:5716-33.
[31] ZHANG Kai GX, HAN Shuai, SUN Leping. Capacity Planning of Power-to-gas Considering Reaction Heat Recovery and Cooperative Game. Power System Technology. 2021.
[32] Wang H, Zhang, C., Li, K., & Ma, X. . Game theory-based multi-agent capacity optimization for integrated energy systems with compressed air energy storage. Energy. 2021;221.
[33] Fang Fang SY, Mingxi Liu. An improved Shapley value-based profit allocation method for CHP-VPP. energy. 2020;213.
[34] Zhongfu Tan CT, Lei Pu, et al. Two-Layer Game Model of Virtual Power Plant Applying CIQPSO Algorithm. Electric Power Construction. 2020;41:9-17.
[35] YANG Shenbo TZ, ZHAO Rui, DE Gejirifu, LI Hongyu, JU Liwei, ZHOU Fengao. Operation optimization and income distribution model of park integrated energy system with power-to-gas technology and energy storage. Journal of Cleaner Production. 2020;247.
[36] Shenbo Yang ZT, Rui Zhao, Gejirifu De, Hongyu Li, Liwei Ju, Feng'ao Zhou. Operation optimization and income distribution model of park integrated energy system with power-to-gas technology and energy storage. journal of cleaner production. 2020;247.

[37] Yuanyuan S. Energy Consumption Modeling and Cruising Range Estimation Based on Driving Cycle for Electric Vehicles: Beijing Jiaotong University; 2014.
[38] CHENG Yaohua DE, TIAN Xu, ZHANG Ning, KANG Chongqing. Carbon Capture Power Plants in Power Systems: Review and Latest Research Trends. Journal of Global Energy Interconnection. 2020;3:339-50.
[39] SUN Huijuan MJ, PENG Chunhua. Coordinated Optimization Scheduling of Multi-region Virtual Power Plant With Wind-power/Photovoltaic/Hydropower/Carbon-capture Units. Power System Technology. 2019;43:4040-9.
[40] Liu Z GS, Yu Y. . Optimal Reactive Power Dispatch Using Chaotic Particle Swarm Optimization Algorithm. AUTOMATION OF ELECTRIC POWER SYSTEMS. 2005;07:53-7.
[41] Tichi SG AM, Nazari ME. Examination of energy price policies in Iran for optimal configuration of CHP and CCHP systems based on particle swarm optimization algorithm. Energy Policy. 2010;38:6240-50.
[42] DE Gejirifu TZ LM, YANG Shenbo, MA Jiale, TAN Qingkun, ZHANG Chen. Bidding Strategy of Wind-storage Power Plant Participation in Electricity Spot Market Considering Uncertainty. Power System Technology. 2019;43:2799-807.
[43] Moradi-Dalvand M. M-IB, Amjady N., Zareipour H., Mazhab-Jafari A. Self-scheduling of a wind producer based on Information Gap Decision Theory. energy. 2015;81:588-600.
[44] TAN Zhongfu TC, PU Lei, YANG Jiacheng. Two-Layer Game Model of Virtual Power Plant Applying CIQPSO Algorithm. Electric Power Construction. 2020;41:9-17.
[45] U.S. Department of Transportation FHA. national household travel survey. 2017.
[46] Xurui H. Power System Optimal Operation with Carbon Capture Plants and Wind Power under Low Carbon Economy: Huazhong University of Science & Technology; 2016.
[47] ZHOU Renjun SH, TANG Xiafei, Zhang Wujun, YU Hu. Low-Carbon Economic Dispatch Based on Virtual Power Plant Made up of Carbon Capture Unit and Wind Power Under Double Carbon Constraint. Proceedings of the CSEE. 2018;38:1675-83.